NANO LETTERS

2007
Vol. 7, No. 9
2707−2710

The Optical Visibility of Graphene: Interference Colors of Ultrathin Graphite on SiO_2

S. Roddaro,* P. Pingue, V. Piazza, V. Pellegrini, and F. Beltram

NEST CNR-INFM & Scuola Normale Superiore, Piazza dei Cavalieri 7, I-56126 Pisa, Italy

Received May 17, 2007

ABSTRACT

Monatomic layers of graphite are emerging as building blocks for novel optoelectronic devices. Experimental studies on a single graphite layer (graphene) are today possible since very thin graphite can be identified on a dielectric substrate using a normal optical microscope. We investigate the mechanism behind the strong visibility of graphite, and we discuss the importance of substrates and of the microscope objective used for the imaging.

Thin graphite has recently attracted renewed interest owing to the possibility to contact single layers and use them as device building blocks.[1−6] A graphite monolayer, also known as graphene, constitutes a rather unique case of a stand-alone two-dimensional electron system with remarkable properties: its mobility is high even at room temperature and both p-type or n-type conduction can be induced by external gating.[1,2,6] In addition, graphene band structure displays a set of very unusual features that allows one to probe interesting transport phenomena such as anomalous integer quantum Hall effects.[3−5]

Graphene samples can be obtained by mechanical exfoliation on a SiO_2/Si substrate.[1,2] This simple technique, however, yields flakes of very different thicknesses: identification of the ultrathin layers on SiO_2/Si can be a crucial step in the fabrication of graphene-based devices. "Good" graphite flakes are often sought for in the first place by using optical microscopy. In fact this technique allows a quick thickness survey before more precise but less direct methods such as Raman spectroscopy[7−9] are used to selectively investigate small portions of the sample. Another important test can stem from the investigation of the anomalous transport behavior expected for single graphene layers,[3,4] but issues related to interlayer coupling in real graphite[10] still cast some doubts on the thickness estimates obtained with this approach. Reports on optical imaging of thin graphite layers have been sometimes controversial as well: in some cases single-layer graphene is said to be invisible,[1,2] while other experiments imply that it can be seen by straightforward optical means.[5] In this Letter we focus on the physics behind the marked visibility of ultrathin graphite on SiO_2/Si substrates and present a simple model that reproduces well the observed graphite colors. Phase shift in the interference color is the most cited mechanism, while our analysis indicates that graphite opacity is the key element in explaining the effect. We shall discuss the importance of the substrate and of the objective employed on the actual graphite visibility. Finally we shall propose possible directions of optimization for techniques relying on optical imaging.

An optical microscope (OM) image of graphite on SiO_2/Si is reported in Figure 1a for a substrate with an oxide thickness $\Delta_{SiO_2} = 500$ nm. This OM picture can be compared with a topographic image obtained using an atomic force microscope (AFM), Figure 1b.[11] A few monolayer thick regions are indicated by a dashed rectangle and are barely visible optically. The same sample was also imaged with a scanning electron microscope (SEM) at low acceleration voltage, Figure 1c.[12] Visibility of thin graphite with SEM can be slightly better than that with OM if one uses the appropriate electron detector and low voltages; however, SEM imaging can be a rather unsuitable technique as it often leads to amorphous carbon deposits on the samples under observation. It appears that AFM can yield the most precise information about graphite thickness, but it is a completely impractical method if one wants to systematically probe large samples. OM imaging does confirm as the most attractive technique for a convenient and large-scale investigation of macroscopic samples. Once the most promising graphite flakes are spotted, different options exist for a more precise thickness evaluation over small areas, as discussed above.

It is well-known that the thickness of a SiO_2 film grown on top of a Si substrate can be quantified with some precision simply by evaluating its apparent color.[13] The latter is in fact due to the interference between the reflection paths that

* Corresponding author. E-mail: s.roddaro@sns.it.

10.1021/nl071158l CCC: $37.00
Published on Web 08/01/2007

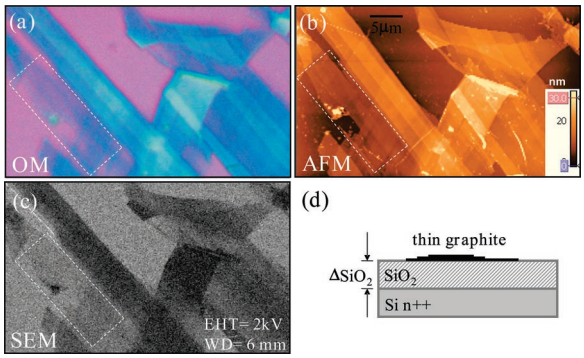

Figure 1. Image of big graphite flake containing regions of many different thicknesses. The pictures were taken using an optical microscope (a), an atomic force microscope (b), and a scanning electron microscope (c). A ultrathin graphite region (thickness below 2 nm) is highlighted by a dashed rectangle. (d) Graphite is deposited on top of a SiO_2/Si substrate with an oxide thickness $\Delta SiO_2 = 500$ nm.

originate from the two air-to-SiO_2 and SiO_2-to-Si interfaces. Depending on their distance, interfering paths will experience relative phase shifts: thickness variations of a fraction of wavelength lead to color shifts that can be easily appreciated by eye. Even within this framework, visibility of thin graphite on SiO_2/Si is striking as it is generally agreed that few monolayers, with a total thickness of the order of 1 nm, can still be identified.[1,2] Such a thickness accounts for barely one or two parts over 1000 of the average wavelength in air for visible light: a remarkably small fraction to be appreciated by the eye, even when phase contrast is involved. Indeed, here we shall argue that such a simple interpretation based on phase shifts is incorrect. We shall show that most of the effect is due a modulation of the relative amplitude of the interfering paths. This is a consequence of the fact that graphite transparency depends on thickness in a sensitive way, since graphite is a good conductor. Relative amplitude modulations are made strongly visible by a favorable combination of permittivity values in the SiO_2/Si multilayer. This leads to a resonant cancellation of reflection by destructive interference at specific wavelengths for finely tuned and relatively thin graphite layers.

In order to explore this mechanism more, we shall analyze the results of a simple bulk model for the multilayer in Figure 1d. The calculation we present is based on classical electrodynamics and on the transfer matrix formalism.[14] This approach is particularly suited for the calculation of transmission and reflection through multiple dielectric layers as shown in Figure 2a. We assume normal incidence with polarization in the $\hat{x}$ direction. Every single layer j is described in terms of a complex dielectric constant ϵ_j and the electric field within a single layer j is

$$E_x = \alpha_j e^{ik_j(z-z_j)-i\omega t} + \beta_j e^{-ik_j(z-z_j)-i\omega t} \qquad (1)$$

where k_j satifies the complex equation $k_j^2/\omega^2 = \epsilon_j \mu_0$ and the causality constraint Im $(k_j) > 0$ and z_j is defined as shown in Figure 2a. The coefficients α_j and β_i quantify the wave components propagating in the positive and negative directions along $\hat{z}$. Coefficients for consecutive layers are linked by Fresnel law which can be also reformulated in terms of matrix multiplication as follows

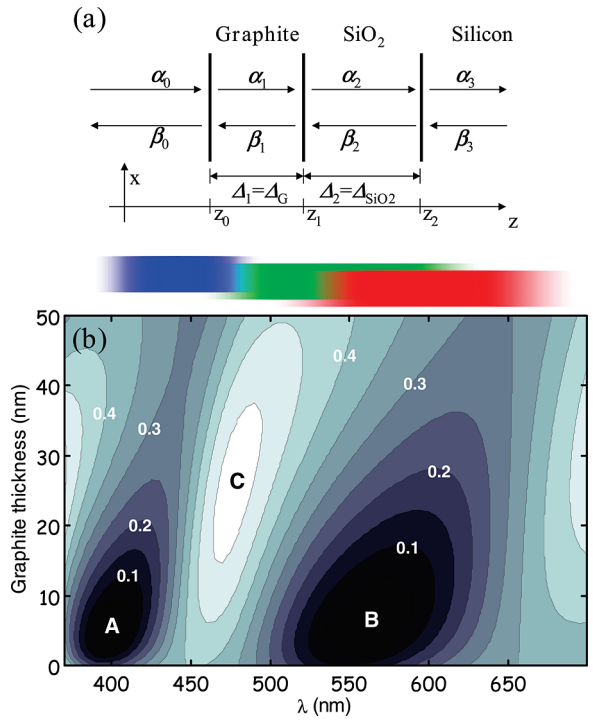

Figure 2. (a) Multilayer structure used in the transfer-matrix simulation. (b) Calculated reflection spectrum $R(\lambda, \Delta_G)$ for a 465 nm thick SiO_2/Si substrate and a variable graphite thickness Δ_G. Due to metallic opacity, graphite modulates the interference contrast in the reflection pattern of the SiO_2 layer: this leads to a set of points of resonant reflection cancellation (A and B) which are intimately linked to the strong optical visibility for thin graphite.

$$\begin{bmatrix}\alpha_{j+1}\\ \beta_{j+1}\end{bmatrix} = \begin{bmatrix}P_+ & 0\\ 0 & P_-\end{bmatrix}\cdot\begin{bmatrix}T_+ & T_-\\ T_- & T_+\end{bmatrix}\cdot\begin{bmatrix}\alpha_j\\ \beta_j\end{bmatrix} \qquad (2)$$

where $P_\pm = e^{\pm ik_{j+1}\Delta_{j+1}}$ for a given layer thickness Δ_{j+1} and $T_\pm = (1 \pm k_j/k_{j+1})/2$. The first matrix starting from the right side describes the transmission and reflection across the interface between the j and $j+1$ layers, the second one the propagation through the $j+1$ layer. The complete transfer matrix M for the multilayer can be obtained by multiplication of such simple matrices. The final transfer equation

$$\begin{bmatrix}\alpha_n\\ \beta_n\end{bmatrix} = \begin{bmatrix}M_{11} & M_{12}\\ M_{21} & M_{22}\end{bmatrix}\cdot\begin{bmatrix}\alpha_0\\ \beta_0\end{bmatrix} \qquad (3)$$

can be used to calculate the global reflection amplitude r in a straightforward way. The configuration of interest here, with an incoming beam from the left of Figure 2a and a reflected and transmitted beams, can be obtained by setting $\beta_n = 0$ (no incidence from the right) and $\alpha_0 = 1$ (unitary incidence from the left). Simple algebra indicates that $r = \beta_0 = -M_{21}/M_{22}$ and the reflection coefficient can be obtained as $R = |r|^2 = |M_{21}/M_{22}|^2$. We adopted standard dielectric constants for air, silicon, and SiO_2.[13] Graphite was described

by $\epsilon_1/\epsilon_0 = 4.5 + 7.5i$, following experimental data in the optical region of the spectrum.[15,16] The latter value yields a skin depth value which is consistent with observations (≈50 nm[1,2]).

Figure 2b displays the main numerical result of the paper: the contour plot of the reflection spectrum $R(\lambda, \Delta_G)$ as a function both of the wavelength $\lambda = 2\pi c/\omega$ and of the graphite thickness Δ_G. The calculation was performed for $\Delta_{SiO_2} = 465$ nm and such a choice will be discussed later in the paper. Very similar results are obtained for different values of Δ_{SiO_2} since the impact of the oxide thickness is mostly to give a shift in the λ position of reflection minima and maxima. Figure 2b shows rather clearly that the presence of thin graphite on the surface produces a red shift of the interference in the reflection spectrum as a consequence of the additional optical length introduced in the system. However Figure 2b also highlights that for $\Delta_G \approx 5$ nm graphite layers strongly *enhance* the interference effects already present at $\Delta_G = 0$ (bare SiO_2/Si substrate) and lead to a resonant suppression of the reflection for specific matching conditions in the (λ, Δ_G) parameter space. For the specific case reported here, we obtain reflection zeros A and B for $\lambda \approx 390$ nm and $\lambda \approx 560$ nm within the visible spectrum and $\Delta_G \approx 5$ nm. This effect is due to a *modulation* of the transparency of the air−graphite−SiO_2 interface which allows the light to reach the SiO_2 layer: only for a finely tuned thickness, Δ_G, it is possible to maximize the interference contrast and meet the conditions for a completely destructive interference in the reflection. The whole system can fruitfully be thought as a sort of Fabry−Perot cavity where graphite plays a role in balancing the input/output barriers. We argue that the presence of these reflection zeros is the main reason for the strong visibility of thin graphite on SiO_2.

Our results match closely the observed color evolution of a real graphite flake. This can be seen directly by converting the spectra reported in Figure 2b into an RGB feed for display device. Red, green, and blue channels can be calculated by appropriate spectral weights (RGB matching functions) as defined by the CIE stardards.[13,17] Panels a and b of Figure 3 compare the real image (color camera Nikon DS-5M and objective Nikon CF Plan 100X with a numerical aperture (N.A.) of 0.8) with the color versus thickness calibration that obtained in our simulation. While any scheme of RBG color reproduction has a fidelity which is structurally limited,[13] such a color scale can serve as an useful "roadmap" to sort out graphite thicknesses and find regions that really have a chance to contain single layers. We note that, given the relatively broad features of the reflection modulation in Figure 2b, much of spectral modulation of Figure 2b can be already seen just by looking at the R, G, and B components of Figure 3a, as reported in panels c, d, and e of Figure 3, respectively. Figure 3f reports a large-scale AFM scan that can be used as a thickness reference. A strong reflection modulation for thin graphite is visible on the red channel which is sampling the $\lambda \approx 500-650$ nm region: R first decreases and then, once Δ_G goes past the minimum B in Figure 2b, it increases again. The green channel, sampling

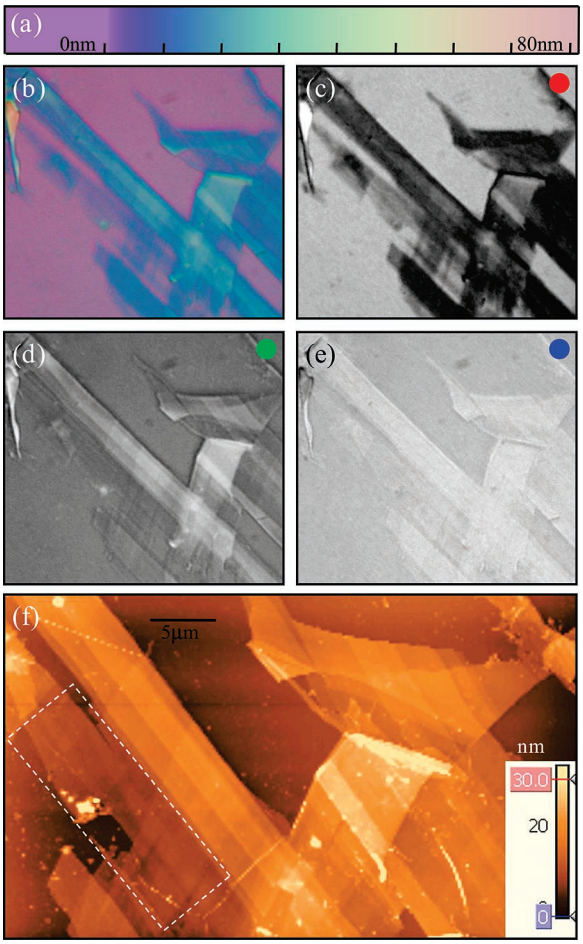

Figure 3. The interference pattern we calculate can be converted into RGB colors (a) and the comparison with the experimentally observed colors (b) is good. The red (c), green (d), and blue (e) components from the same image reproduce the main features of our numerical result in Figure 2b. While image (b) was not modified in any way, contrast on panels c, d, and e was maximized for better visibility. (f) Large-scale atomic force scan for thickness reference.[11]

the range $\lambda \approx 450-600$ nm is mostly displaying an increased reflection with increasing graphite thickness, as expected by the presence of the maximum C. The blue channel ($\lambda \approx 400-500$ nm) does not show any particular variation in the reflection intensity as this spectral region is just at the transition between the minimum A and the maximum C.

Having clarified the origin of the phenomenon leading to graphene visibility, we now focus on the intrinsic limits of thickness evaluation by OM and provide guidelines for improvement. A crucial issue to take into account is that incidence and reflection of light on the sample are *not* orthogonal in the OM: optical beams are in fact conical, as quantified by the numerical aperture of the microscope objective. Therefore different interference patterns will be obtained depending on the incidence angle and light polarization and these will sum up incoherently in the microscope due to the typical poor coherence of the exploited light sources. Features in Figure 2b will thus be smoothed out and the visibility of thin graphite on SiO_2 will eventually decrease. Such an effect can be quantified by taking for example our objective with N.A. = 0.8. The maximum

deviation angle between the optical beams and the perpendicular direction within the oxide layer will be ≈30°. This will generally lead to a complex light averaging; however, as long as one neglects the angle dependence of the reflectivity of the interfaces and considers a geometric optics approach, it is easy to show that for a beam traveling at an angle θ through the multilayers interference patterns will just shift as if due to an effective oxide thickness $\Delta_{SiO_2,eff} = \Delta_{SiO_2} \cos\theta$. This is rather important in reproducing correctly the observed colors: by using nominal Δ_{SiO_2} values from our wafers we can easily reproduce[13] the color observed by eye (N.A. $\ll$ 1); however, the same wafer observed through an OM will look rather different. The color shift is partly due to the different lighting conditions but also related to the large N.A. of the microscope objectives that are typically used, as one can easily verify by comparing colors observed with different objectives. A simple average of the cosine value assuming a uniform lighting of the objective lens yields $\langle\cos\theta\rangle \approx 0.92$ for our N.A.: in agreement with this, graphite colors of Figure 1a could be reproduced using $\Delta_{SiO_2} = 465$ nm. Similar calculations performed at $\Delta_{SiO_2} = 230$ nm can reproduce, in a completely equivalent way, apparent colors observed on substrates with 250 nm thick oxide layers.[18] Our analysis also suggests possible directions for improving this technique. We expect, in fact, that a smaller N.A. will increase the contrast of thin graphite even though the image details will probably be negatively affected. An improvement should be observed when using more refractive dielectric media such as Si_3N_4 as this will decrease the incidence angle in the dielectric medium and the averaging effect discussed above. On the other hand Si_3N_4, being characterized by a different dielectric constant, will present reflection zeros for different positions in the (Δ_G, λ) space and the contrast of thin graphite will be affected. Light coherence, in particular in the regions of the spectrum interested by the reflection minima could also be useful in reducing the incoherent averaging linked to a large N.A.

Concerning preferential values for the oxide thickness Δ_{SiO_2}, our analysis indicates that interference effects will always be present regardless the value of Δ_{SiO_2}. The thickness of the oxide will just determine the frequency position of the reflection zeros of Figure 2b while the effect will remain qualitatively the same. On the other hand, as long as graphite is observed by eye or using a standard trichromatic color camera, interference patterns will be more or less *visible* depending on the details of human eye sensitivity.[19] On the basis of our experience we find that our 500 nm substrate gives a good visibility of thin graphite. As shown here, graphite colors observed on such a substrate agree with the presence of a reflection minimum at $\lambda \approx 550-600$ nm in the red−green portion of the visible spectrum. We expect a similar reflection minimum also for $\Delta_{SiO_2} \approx 300$ nm, usually cited as a "good" oxide thickness for the observation of thin graphite.[1−3] It is important to note that the oxide thickness values used in simulations needs to be corrected when a very large N.A. is used for the imaging. For instance we find that in our case of N.A. = 0.8 a $\Delta_{SiO_2} \approx -7\%$ off the nominal value yields the best reproduction of the observed color scale.

In conclusion, we have discussed the electrodynamics behind the visibility of few monolayers of graphite deposited on thin SiO_2 and we have showed that the visibility of thin graphite is linked to a strong amplitude modulation of reflection at the air−graphite−SiO_2 interface, while the modulation of the optical lengths appears to play a marginal role. Finally we note that a simple extrapolation from our model yields a reduction of reflection between $\Delta_G = 0$ (bare substrate) and $\Delta_G = 0.34$ nm (thickness of single-layer graphene) in excess of 10% in the spectral regions corresponding to the minima in Figure 2. Once issues related to N.A. are solved or kept under control, such a color modulation could be easily detectable and effectively used for a reliable thickness evaluation of ultrathin graphite.

Supporting Information Available: Figures showing real versus simulated colors on different SiO_2 substrates. This material is available free of charge via the Internet at http://pubs.acs.org.

References

(1) Novoselov, K. S.; Jiang, D.; Schedin, F.; Booth, T. J.; Khotkevich, V. V.; Morozov, S. V.; Geim, A. K. *Proc. Natl. Acad. Sci. U.S.A.* **2005**, *102*, 10451.
(2) Novoselov, K. S.; Geim, A. K.; Morozov, S. V.; Jiang, D.; Zhang, Y.; Dubonos, S. V.; Grigorieva, I. V.; Firsov, A. A. *Science* **2004**, *306*, 666.
(3) Novoselov, K. S.; Geim, A. K.; Dubonos, S. V.; Hill, E. W.; Grigorieva, I. V. *Nature* **2005**, *438*, 197.
(4) Novoselov, K. S.; McCann, E.; Morozov, S. V.; Fal'ko, V. I.; Katsnelson, M. I.; Zeitler, U.; Jiang, D.; Schedin, F.; Geim, A. K. *Nat. Phys.* **2006**, *2*, 177.
(5) Zhang, Y.; Tan, Y.-W.; Stormer, H. L.; Kim, P. *Nature* **2005**, *438*, 201.
(6) Heersche, H. B.; Jarillo-Herrero, P.; Oostinga, J. B.; Vandersypen, L. M. K.; Morpurgo, A. F. *Nature* **2007**, *446*, 56.
(7) Ferrari, A. C.; Meyer, J. C.; Scardaci, V.; Casiraghi, C.; Lazzeri, M.; Mauri, F.; Piscanec, S.; Jiang, D.; Novoselov, K. S.; Roth, S.; Geim4, A. K. *Phys. Rev. Lett.* **2006**, *97*, 187401.
(8) Gupta, A.; Chen, G.; Joshi, P.; Tadigadapa, S.; Eklund, P. C. *Nano Lett.* **2006**, *6*, 2667.
(9) Graf, D.; Molitor, F.; Ensslin, K.; Stampfer, C.; Jungen, A.; Hierold, C.; Wirtz, L. *Nano Lett.* **2007**, *7*, 238.
(10) Lu, Y.; Muñoz, M.; Steplecaru, C. S.; Hao, C.; Bai, M.; Garcia, N.; Schindler, K.; Esquinazi, P. *Phys. Rev. Lett.* **2006**, *97*, 076805.
(11) Image acquired by a NTEGRA microscope, courtesy of NT-MDT.
(12) Image acquired by a LEO 1525 microscope using a standard secondary electron detector.
(13) Henrie, J.; Kellis, S.; Schultz, S. M.; Hawkins, A. *Opt. Express* **2004**, *12*, 1464.
(14) Born M.; Wolf E. *Principles of Optics*; Cambridge University Press: London, 1998.
(15) Taft, E. A.; Philipp, H. R. *Phys. Rev.* **1965**, *138*, A197.
(16) Pedersen, T. G. *Phys. Rev. B* **2003**, *67*, 113106.
(17) ISO/CIE 10527: Colorimetric Observers, 1991. http://www.cie.co.at/cie/.
(18) Supporting Information.
(19) Gegenfurtner, K. R. *Nat. Rev. Neurosci*. **2003**, *4*, 563.

NL071158L